University of Wollongong
Research Online

Australian Institute for Innovative Materials - Papers

Australian Institute for Innovative Materials

2006

Growth of width-controlled nanowires MnO2 from mesoporous carbon and investigation of their properties

Shenmin Zhu
Shanghai Jiao Tong University, China

Xiaolin Wang
University of Wollongong, xiaolin@uow.edu.au

Wei Huang
Shanghai Jiao Tong University, China

Deyue Yan
Shanghai Jiao Tong University, China

Honghua Wang
Shanghai Jiao Tong University, China

See next page for additional authors

Publication Details

Zhu, S, Wang, X, Huang, W, Yan, D, Wang, H & Zhang, D (2006), Growth of width-controlled nanowires MnO2 from mesoporous carbon and investigation of their properties, Journal of Materials Research, 21(11), pp. 2847-2854.

Research Online is the open access institutional repository for the University of Wollongong. For further information contact the UOW Library: research-pubs@uow.edu.au

Growth of width-controlled nanowires MnO2 from mesoporous carbon and investigation of their properties

Abstract

One-dimensional α-MnO_2 nanowires with a controlled width of 10–20 nm have been developed by means of ultrasonic waves from mesoporous carbon using $KMnO_4$ as the precursor. The formation mechanism has been proposed based on the results. A peak around 100 K was detected in the temperature-dependence of magnetization curve, indicating the ferromagnetic state in nanocomposite mesoporous carbon-MnO_2, which is in agreement with the transition temperature found from the magnetization versus applied magnetic field curve. The magnetization versus temperature curve of the obtained MnO_2 nanowires showed a magnetic transition at about 50 K, illustrating that a parasitic ferromagnetic component is composed on the antiferromagnetic structure of MnO_2. The advantage of the method reported here is that phase-controlled synthesis of α-MnO_2 nanowires was implemented regardless of pH, temperature, and types of ions in the reaction system. A major advantage of this approach is the efficient, fast, and reproducible control of width and the facile strategy to synthesize nanowires MnO_2, in addition to the high purity of the resultant material.

Keywords

Growth, width, controlled, nanowires, MnO2, from, mesoporous, carbon, investigation, their, properties

Disciplines

Engineering | Physical Sciences and Mathematics

Publication Details

Zhu, S, Wang, X, Huang, W, Yan, D, Wang, H & Zhang, D (2006), Growth of width-controlled nanowires MnO2 from mesoporous carbon and investigation of their properties, Journal of Materials Research, 21(11), pp. 2847-2854.

Authors

Shenmin Zhu, Xiaolin Wang, Wei Huang, Deyue Yan, Honghua Wang, and Di Zhang

This journal article is available at Research Online: http://ro.uow.edu.au/aiimpapers/256

Growth of width-controlled nanowires MnO_2 from mesoporous carbon and investigation of their properties

Shenmin Zhu[a)]
State Key Laboratory of Metal Matrix Composites, Shanghai Jiao Tong University, Shanghai 200030, People's Republic of China

Xiaolin Wang
Spintronic and Electronic Materials Group, Institute for Superconducting and Electronic Materials, University of Wollongong, New South Wales 2522, Australia

Wei Huang, Deyue Yan, Honghua Wang, and Di Zhang
Coll. Chem. & Chem. Eng., State Key Lab Met Matrix Composites, Shanghai Jiao Tong University, Shanghai 200030, People's Republic of China

(Received 16 March 2006; accepted 23 June 2006)

One-dimensional α-MnO_2 nanowires with a controlled width of 10–20 nm have been developed by means of ultrasonic waves from mesoporous carbon using $KMnO_4$ as the precursor. The formation mechanism has been proposed based on the results. A peak around 100 K was detected in the temperature-dependence of magnetization curve, indicating the ferromagnetic state in nanocomposite mesoporous carbon-MnO_2, which is in agreement with the transition temperature found from the magnetization versus applied magnetic field curve. The magnetization versus temperature curve of the obtained MnO_2 nanowires showed a magnetic transition at about 50 K, illustrating that a parasitic ferromagnetic component is composed on the antiferromagnetic structure of MnO_2. The advantage of the method reported here is that phase-controlled synthesis of α-MnO_2 nanowires was implemented regardless of pH, temperature, and types of ions in the reaction system. A major advantage of this approach is the efficient, fast, and reproducible control of width and the facile strategy to synthesize nanowires MnO_2, in addition to the high purity of the resultant material.

I. INTRODUCTION

The controlled syntheses of metal oxides, especially those that are supposed to present some novel properties with a particular dimensionality and size, has attracted intensive attention.[1] MnO_2 has been the focus of material scientists because of its advanced applications in molecular sieves, catalysts, and lithium batteries.[2,3] Synthesis of one-dimensional MnO_2 with controlled width is of great interest because the low-dimensional structure results in an improved electrochemical performance, as well as in unique nanomagnetic properties.[4] Several successful techniques have been reported in the synthesis of one-dimensional nanostructures, such as thermal evaporation,[5] nanotube-based synthesis,[6–8] solution-based synthesis,[9] microemulsion,[10] vapor-liquid-solid growth,[11] hydrothermal method,[12] and mesoporous confinement.[13–17] In comparison with soft chemical processes,[18] the hard-templating process is a very different approach that has attracted considerable attention. Direct nanocasting of mesoporous silica has been used widely for the preparation of metal oxide nanowires, including nanocrystallites β-MnO_2.[19,20] Highly ordered mesoporous carbon (CMK-3) with its regular array of uniform mesopores exhibits not only thermal and mechanical stability, but also the capability of enduring various chemical solutions. Mesoporous spheres of several metal oxides have been synthesized from mesoporous carbon[21,22] via the traditional wet impregnation method. Previously, β-MnO_2 nanowires have been prepared from SBA-15 via the "two-solvent" method using low-oxidation-state $Mn(NO_3)_2$ as the precursor.[23] However, no article has appeared concerning MnO_2 nanowires from mesoporous carbon. In fact, the chemical nature and dimensions of metal oxide nanowires are affected by the characteristics of the precursor, the structural parameters of the host, and the method of bringing the salt into contact with the host.

We believe that an investigation of the nature and properties of manganese oxide nanowires made from

[a)]Address all correspondence to this author.
e-mail: smzhu@sjtu.edu.cn
DOI: 10.1557/JMR.2006.0356

 © 2006 Materials Research Society

CAMBRIDGE JOURNALS
http://journals.cambridge.org Downloaded: 09 Oct 2012 IP address: 130.130.37.84

mesoporous carbon using a high-oxidation-state $KMnO_4$ precursor would be of considerable interest. Recently, we described the preparation of MnO_2 nanoparticles inside channels of mesoporous carbon using a sonochemical method.[24] This suggested the possibility of obtaining one-dimensional MnO_2 from nanocomposites of MnO_2 inside hexagonal mesoporous carbon (CMK-MnO_2). Herein, we report a simple approach for the preparation of width-controlled MnO_2 nanowires using CMK-3 as the template and we propose a formation mechanism from analysis of the results. Unsupported MnO_2 nanowires were obtained by removal of the carbon using a thermal treatment at 550 °C in air for 6 h. The unique magnetic properties for CMK-MnO_2 nanocomposite and MnO_2 nanowires are presented and discussed. Moreover, the presence of carbon is reported to favor the formation of nanowires,[20] which enable CMK-3 to be an ideal host for synthesizing width-controlled metal oxide nanowires with potential applications in optical, electronic, and magnetic nanodevices.

II. EXPERIMENTAL SECTION

A. Material synthesis

The synthesis of self-ordered hexagonal mesoporous silica SBA-15 is the same as described under acid conditions. The process of producing mesoporous carbon is similar to that described by Ryoo.[25,26] MnO_2 incorporation into carbon CMK-3 was achieved in the following way: 0.3 g of mesoporous carbon CMK-3 was treated with concentrated H_2SO_4 at 80 °C for 3 h and was then washed with deionized water and dried at 80 °C. Successful surface modification was verified by Fourier-transformed infrared (FTIR) analysis with the appearance of a new band at 1716 cm^{-1}, typical of the carboxylic moiety (–COOH). Modified CMK-3 (0.1 g) was then dispersed into a concentrated aqueous solution of $KMnO_4$ (0.03 M). Two hours later, the mixture was subjected to ultrasound at room temperature in the form of 100 Hz ultrasonic waves at 600 W output power. During irradiation, water flow was used to control the glass vessel in the bath. After 8 h of irradiation, the precipitate was filtered, washed thoroughly with distilled water, and dried at 120 °C for 10 h. The samples thus prepared are referred to as CMK-MnO_2-8. Unsupported MnO_2 nanowires were obtained by removal of the carbon via combustion at 550 °C in air for 6 h (MnO_2). As a comparison, the sample of CMK-MnO_2 heat treated at 450 °C for 2 h in air is referred to C-MnO_2-8. Two additional samples prepared with 6 and 4 h of ultrasonic treatment were donated to be CMK-MnO_2-6 and CMK-MnO_2-4, respectively. Accordingly, unsupported MnO_2 nanowires from CMK-MnO_2-6 and CMK-MnO_2-4 are referred to MnO_2-6 and MnO_2-4, respectively.

B. Material characterization

Powder x-ray diffraction (XRD) patterns were recorded on an x-ray diffractometer system (AXS; Bruker, Billerica, MA) with Cu Kα radiation. Nitrogen adsorption measurements at 77 K were performed on an ASAP2100 volumetric adsorption analyzer, and samples were out-gassed for 8 h in the degas port of the adsorption apparatus. Transmission electron microscopy (TEM) and energy-dispersive x-ray (EDX) measurements were carried out on a 2010 microscope (JEOL, Tokyo, Japan) and a 2100F microscope (JEOL).

III. RESULTS AND DISCUSSION

The relatively good elimination of the template is revealed by elemental analysis (as the carbon content was about 0.9%). EDX measurements with TEM show that the resultant MnO_2 consists of Mn and O with an atomic ratio of about 1:2. This further confirms the almost complete removal of the carbon template from MnO_2 nanowires.

CMK-MnO_2-8 together with unsupported MnO_2 nanowires was characterized with XRD, demonstrated in Fig. 1. One intense diffraction peak in small-angle XRD patterns, which is designated as (100), is observed for CMK-3 and CMK-MnO_2-8, which is characterized by a hexagonal structure. The loading amount of MnO_2 on the CMK-MnO_2-8 was estimated to be 51 wt% from thermogravimetric analysis measured in air. The 51 wt% filling of the porosity with MnO_2 may explain the intensity decrease for the sample of CMK-MnO_2-8 (Fig. 1) in comparison with CMK-3. No peak can be detected for the sample of unsupported MnO_2, which suggests that nanowires with an ordered mesoporous structure do not form.

From high-angle XRD patterns, the obtained MnO_2

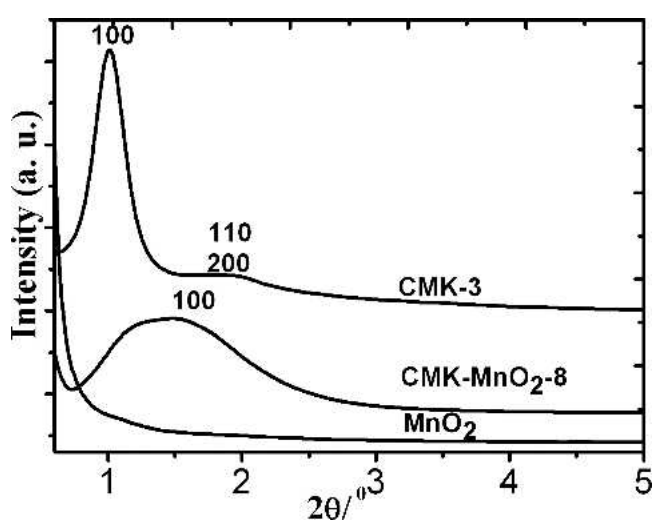

FIG. 1. Small-angle XRD patterns of CMK-3, CMK-MnO_2, and α-MnO_2 nanowires.

CAMBRIDGE JOURNALS
http://journals.cambridge.org Downloaded: 09 Oct 2012 IP address: 130.130.37.84

nanowires were proved to be mainly α-MnO_2. EDX measurements indicated an almost constant atomic Mn/O ratio of 0.5 all over the samples. Davidson[15] considered that the morphology and chemical nature of the resultant nanowires were affected by the precursors and the methods used, as well as by the nature of the host. Zhao[10] obtained a mixture of MnO_2, Mn_2O_3, and Mn_3O_4 nanowires from microwave-digested SBA-15. In contrast, pure β-MnO_2 was synthesized via the "two-solvent" method by Davidson[15] using the same precursor as that of Zhao. In our case, one-dimensional α-MnO_2 nanowires with a controlled width of 10–20 nm were prepared. The factors of high-oxidation-state $KMnO_4$ precursor, surface modification of the CMK-3 to be hydrophilic and ultrasonic waves used made contributions to the formation of α-MnO_2.

The structure and morphology of the nanocomposites CMK-MnO_2-8 were further characterized by TEM. As shown in Figs. 2(b) and 2(c), the nanosized particles of MnO_2 appear as dark rod-like objects before removal of the carbon template, and are distinctly observed to be diffusing very well inside the pores of CMK-3 [Figs. 2(b) and 2(c)] compared with the original CMK-3 [Fig. 2(a)]. The diameter of the nanowires is about 3 nm inside the carbon mesopores, which is consistent with the diameter of CMK-3 (around 3.9 nm, as determined by N_2 adsorption/desorption).

The TEM images in Fig. 3(a) reveal the formation of large number nanowires for the sample of unsupported MnO_2. From the high resolution transmission electron microscopy (HRTEM) images, we can detect the existence of a large amount of nanowires with an average width around 10–20 nm [Fig. 3(b)]. The high magnification images display very well crystal nanowires, and the lattice fringes correspond to *d*-spacing of 0.701 nm, characteristic of α-MnO_2 [Fig. 3(c)]. These are in agreement with the d_{110}-spacing observed in XRD patterns of MnO_2 nanowires. It is known that variety factors exist to influence the growth of MnO_2 one-dimensional nanostructures, such as the concentration of ions, temperature, pH, etc. In the past, people tried to control the morphology of the final products by adding ions or adjusting pH or temperature. Herein, phase-controlled synthesis of α-MnO_2 nanowires can be realized via an easy sonochemical method. As is mentioned above, the pore diameter of the original CMK-3 was determined to be about 3.9 nm via nitrogen adsorption/desorption analysis. The questions then arise: is the width of MnO_2 nanowires thus prepared larger than the pore diameter of the original host CMK-3? Are the MnO_2 nanowires formed inside mesopores as we suggested? To find out the truth, HRTEM images were taken as a comparison for the sample of CMK-MnO_2-8 after being heat treated in air at 450 °C for 2 h (C-MnO_2-8), from which it is interesting to find the formation of carbon nanotubes with metal

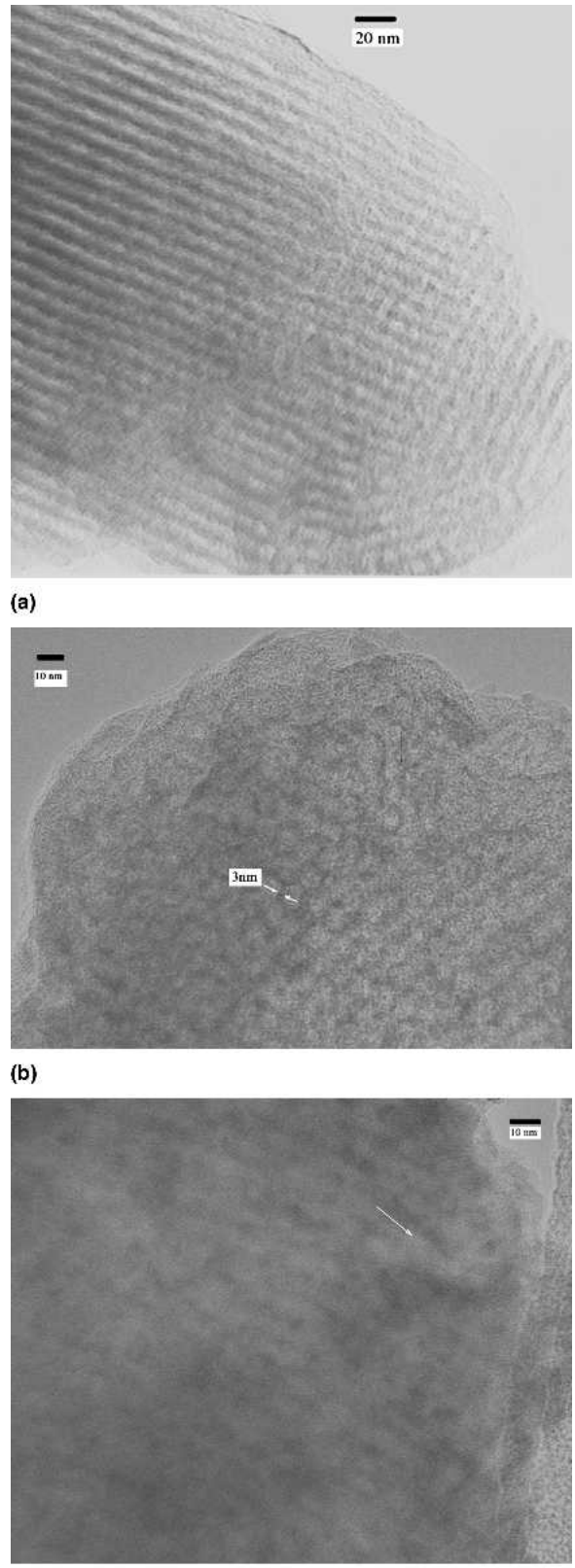

FIG. 2. TEM images of (a) the original CMK-3, (b) CMK-MnO_2 perpendicular to the pore channels, and (c) along the pore channels.

CAMBRIDGE JOURNALS
http://journals.cambridge.org Downloaded: 09 Oct 2012 IP address: 130.130.37.84

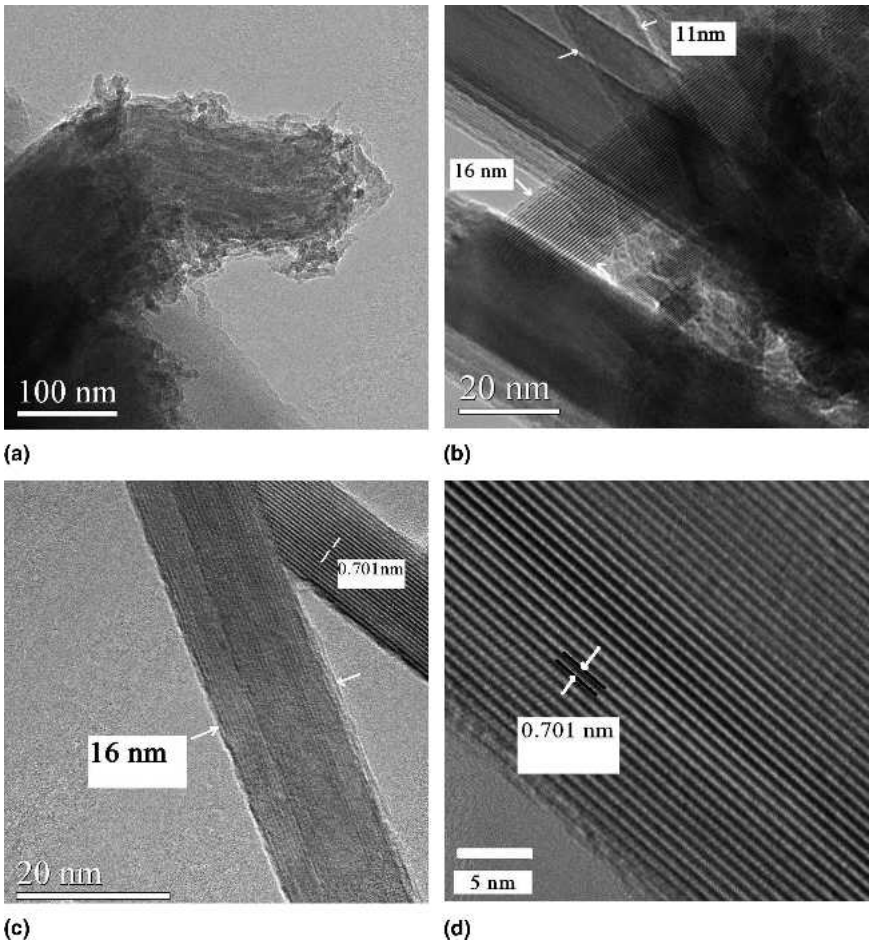

FIG. 3. HRTEM images of the α-MnO_2 nanowires (a) and (b) with the diameters of 10–20 nm, and HRTEM images of α-MnO_2 nanowires, (c) and (d) spacing $d = 0.701$ nm.

oxide aggregation inside the tubes. The process can be detected and illustrated from Fig. 4.

The nanowires were produced from the original CMK-MnO_2-8 by the following process. The micropoles that connected the mesopores of CMK-3 were first combusted as the temperature increased, leaving the individual nanotube-like poles in place [Fig. 4(a)]. Meanwhile, MnO_2 nanoparticles that were previously independent aggregated along the pore channels inside the pores and crystallized as the temperature increased [Fig. 4(a)]. Thus, nanocomposite C-MnO_2-8 consists of two parts: one part consists of the dark rod-like objects inside and the other consists of the gray walls outside. Spectra obtained from EDX verified that the dark rod-like objects inside the tube were composed of pure MnO_2 [Fig. 4(b)]. The gray part is mainly made up of carbon, with only 0.4% Si and S [Fig. 4(c)] and 0.48% of impurity Ca; no Mn was detected. A more highly resolved TEM image gives further evidence of the core-shell structures from Fig. 4(d), which clearly reveals the lattices of the nanowires inside and the layer distance of 0.34 nm for the gray wall corresponding to the graphite structure.

As demonstrated in Fig. 4(a), the carbon wall was reduced to 3 nm from the original 6 nm via combustion, and the width of the MnO_2 nanowires expanded accordingly to 9 nm, occupying the original wall position. The width of an entire nanowire is about 15 nm, which is consistent with the calculated distance between two carbon poles (pore diameter 3.9 nm + twice carbon walls 12 nm = 15.9 nm). The proportion of the MnO_2 content inside the host expands as the wall becomes thinner and thinner. Finally, the widths of the nanowires reach 10–20 nm with perfect crystalline phase owing to the high temperature [Fig. 3(b)]. The structures of the nanowires thus prepared are different from those in the report on β-MnO_2 fabricated from nanocasting of SBA-15,[15] which indicated that the width of the metal nanowires is almost equal to the original host pore diameter.[10] A different formation mechanism can explain these results. The silica framework can be dissolved using a solution of HF/H_2O/EtOH or NaOH. Nevertheless, carbon cannot be removed by the conventional solution because of its inactive properties. During the removal of carbon template at high temperatures, the nanowires widened to

CAMBRIDGE JOURNALS
http://journals.cambridge.org Downloaded: 09 Oct 2012 IP address: 130.130.37.84

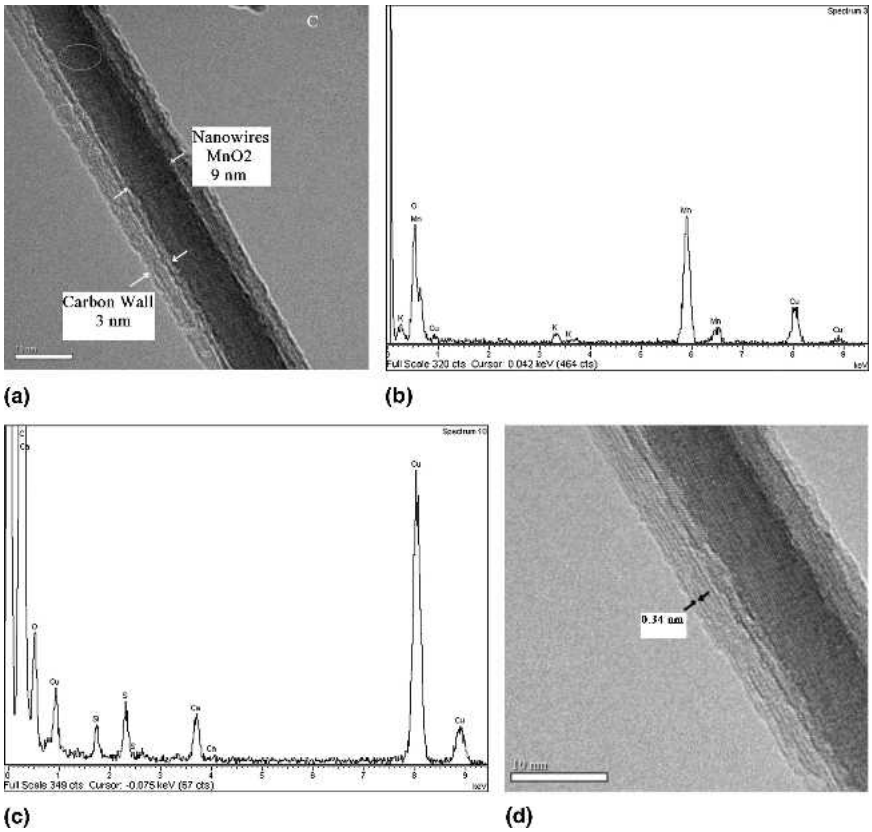

FIG. 4. HRTEM images of (a) nanocomposite C-MnO_2 (CMK- MnO_2 heat-treated at 450 °C in air for 2 h; (b) EDX measurement taken at the position of the black rod-like objects inside the tube in (a); (c) EDX measurement taken at the gray wall in image (a). (d) HRTEM image gives further evidence of the core-shell structures, which clearly reveals the lattices of the MnO_2 nanowires inside and the layer distance of 0.34 nm for the gray wall corresponding to the graphite structure.

occupy the position of the carbon removed and thus aggregated in one dimension, resulting in samples with the diameter of the mesoporous pores plus one or two wall thicknesses.

Xiao et al.[27] have proposed that the hollandite-type MnO_2 random weave nanofibrous structure develops from an initial nanoparticle agglomerated mass under the reflux conditions. Here, we believe the mesostructures of the template, ultrasonic sound, and combustion are responsible for the formation of α-MnO_2 nanowires. The formation process can be described as follows as described in Scheme 1: The surface modification of CMK-3 (to become hydrophilic with –COOH) makes it easy for $KMnO_4$ to access the pore channels of CMK-3. At the same time, modification changes the surface reactivity, enabling the formation of MnO_2 nanoparticles inside the pores of CMK-3 by sonochemical reduction of metal ions. Small particles are pushed by the jets generated by ultrasound waves, and are anchored to the inner surface of the mesoporous carbon. MnO_2 nanoparticles inside the mesopores aggregate along the channels of the mesopores at elevated temperatures. As the process continues, the carbon wall is burned up in air and becomes thinner and thinner. The aggregation of the MnO_2 nanoparticles gets wider and wider, occupying the position of the burned carbon. Finally, one-dimensional MnO_2 nanowires are synthesized with a controlled width of 10–20 nm.

Two additional experiments were conducted to investigate the effect of the loading amount of MnO_2 on the size of nanowires. Figure 5 shows the wide-angle XRD patterns of nanowires MnO_2 prepared from different CMK-MnO_2 with various loading amounts by varying irradiation time. The sample of CMK-MnO_2-8 has the

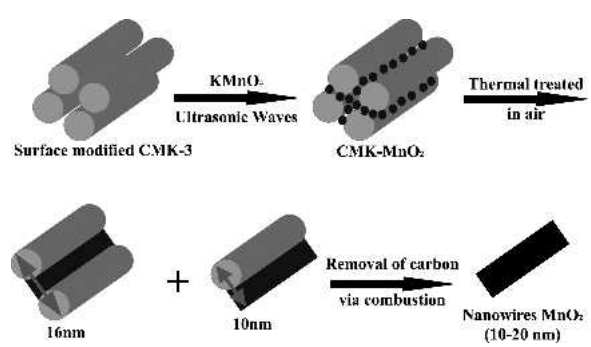

SCHEME 1. The mechanism responsible for the formation of MnO_2 nanowires from a mesoporous carbon template.

CAMBRIDGE JOURNALS
http://journals.cambridge.org Downloaded: 09 Oct 2012 IP address: 130.130.37.84

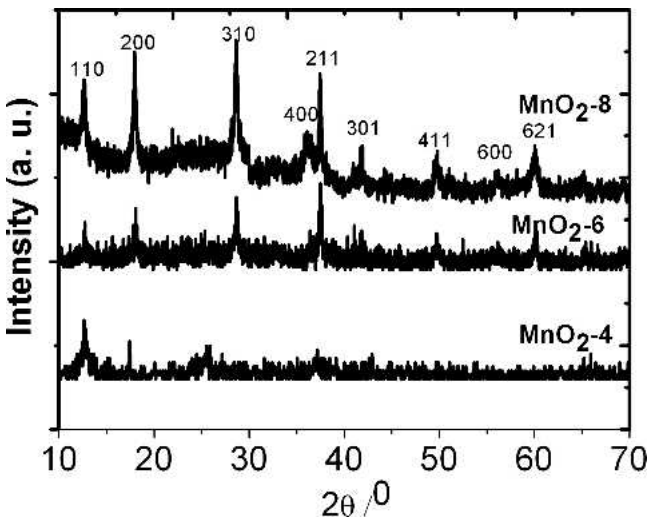

FIG. 5. The wide-angle XRD patterns of nanowires MnO_2 prepared from CMK-MnO_2 with various loading amounts by varying irradiation time.

highest MnO_2 loading up to 51 wt%. CMK-MnO_2-4 and CMK-MnO_2-6 are 30 and 43 wt%, corresponding to the samples irradiated for 4 and 6 h, respectively (thermogravimetric analysis not shown). Accordingly, the nanowires with the carbon removed were named MnO_2-4 and MnO_2-6, respectively. MnO_2-6 and MnO_2-8 contained full sites of peaks corresponding to pure crystal nanowire α-MnO_2. The relatively strong intensity in MnO_2-8 compared with MnO_2-6 is attributed to the perfect crystallites of the formation MnO_2 nanowires with a high loading weight. Only broader and less intensive peaks were detected in the MnO_2-4 sample because of its relatively small grain size and the many crystal defects. Similar phenomena have been described in the synthesis of MnO_2-δ nanowire microspheres.[4] That is to say, the controlling width of nanowires is related to the loading amount of MnO_2, in addition to the gradual reduction of carbon wall size during combustion. Low loading amounts result in small-sized nanowires with many defects, owing to the limited amount of MnO_2 that can be aggregated. As the loading amount of MnO_2 increased, nanowires with perfect nanocrystallites increased. Width-controlled nanowires were obtained only when the proper amount of MnO_2 (above 40%) was incorporated inside CMK-3. Therefore, nanowire formation is governed by the aggregation process, starting from statistically dispersed individual nanoparticles in mesopores under thermal treatment. Thus, after removal of the carbon template via combustion, samples with the diameter of the mesoporous pores plus one or two carbon wall thicknesses were prepared. Conversely, it further confirmed that the nanowires MnO_2 formed are indeed grown from the mesopores of carbon. It is worth emphasizing that during this period, two kinds of tubes formed: one with a carbon wall on two sides and the other with a carbon wall on only one side. Another point that should be mentioned is that a few of the nanowires were found to be a little larger than 16 nm, possibly because of agglomeration outside the channels; a similar phenomenon has been reported by Liu.[28] Nitrogen desorption/adsorption depicted in Fig. 6 demonstrates a high surface area of 87 $m^2\ g^{-1}$ for the resultant MnO_2 nanowires.

From the analysis above, we can reach the conclusion that samples of one-dimensional nanowires of α-MnO_2 with diameters of 10–20 nm and a smooth texture can be prepared from mesoporous carbon. The vast majority of the nanowires could be controlled in the typical α-structure. The advantage of our method is that we can get α-MnO_2 directly without any concerns about the process. No additional ions are added, and high purity can be expected.

The magnetic properties of CMK-MnO_2 and MnO_2 nanowire samples were studied by measuring dc and ac magnetization and magnetic hysteresis loops using a commercial Physical Property Measurement System (Quantum Design, San Diego, CA). Figure 7 shows the temperature dependence of the ZFC and FC magnetizations for CMK-MnO_2.

It can be seen that an irreversibility between ZFC and FC starts at around 75–100 K, indicating the formation of a ferromagnetic phase below this temperature range. An ac susceptibility measured in 1 Oe and 117 Hz is shown as the inset in Fig. 7(a). A peak in the ac susceptibility is observed around 100 K in agreement with the transition temperature observed from dc magnetization measurements. The peak in the ac susceptibility indicates an antiferromagnetic interaction or a spin glass state coexisting with the ferromagnetic state in the CMK-MnO_2. The ferromagnetic state can also be seen from magnetic hysteresis loops as shown in Fig. 8(a). An antiferromagnetic

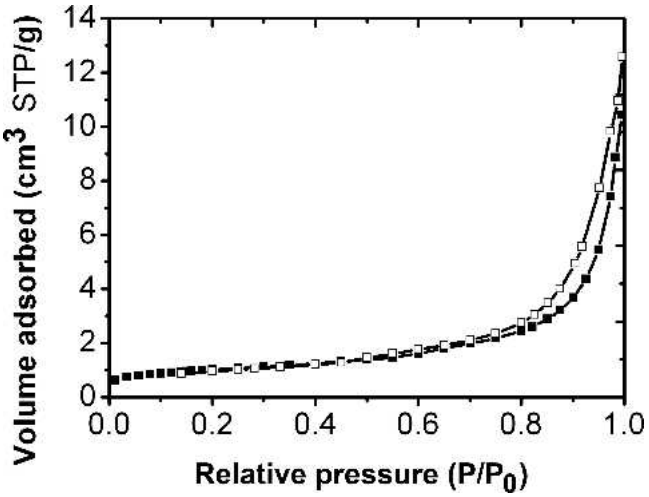

FIG. 6. Nitrogen adsorption/desorption isotherms (at 77 K) of the obtained nanowires MnO_2.

CAMBRIDGE JOURNALS
http://journals.cambridge.org Downloaded: 09 Oct 2012 IP address: 130.130.37.84

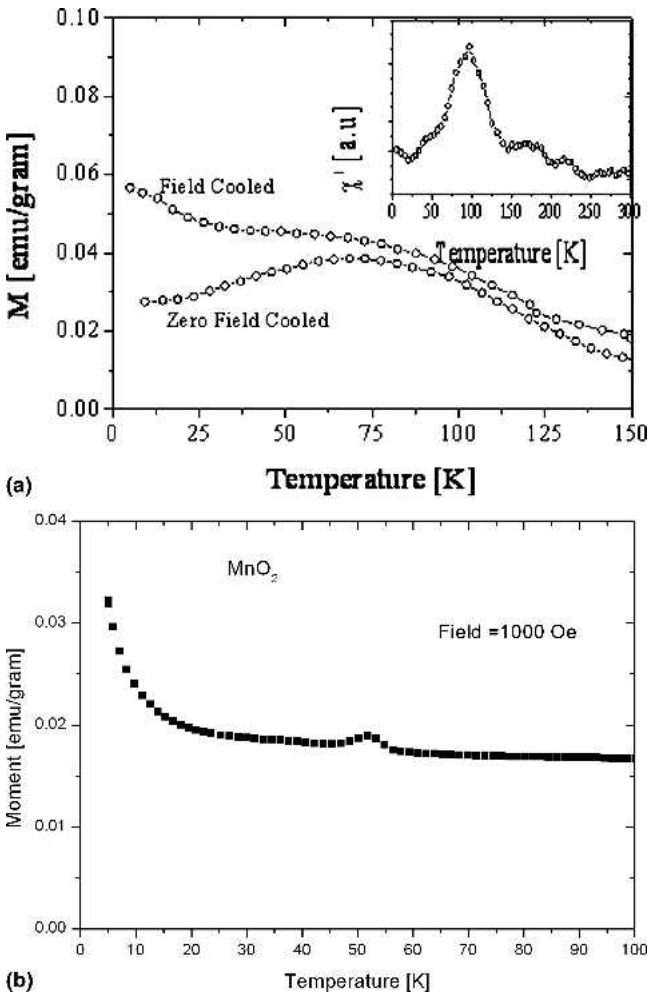

FIG. 7. The temperature dependence of the magnetization curves under zero field cooling (ZFC) and field cooling (FC) for the (a) CMK-MnO_2 and (b) MnO_2 nanowires.

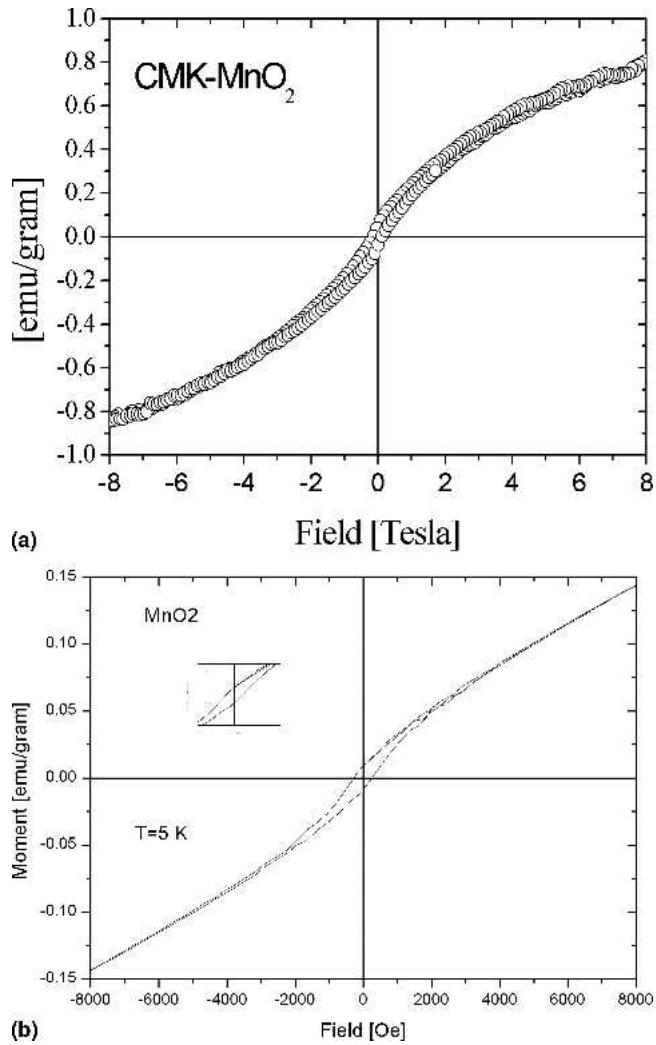

FIG. 8. The field dependence of magnetization of (a) CMK-MnO_2 and (b) MnO_2 nanowires at T = 5 K.

interaction component is present, as the magnetization tends to remain unsaturated, even in high fields of up to 8 T. The temperature dependence of the FC magnetization for a sample of MnO_2 nanowires is shown in Fig. 7(b). A kink is observed at about 50 K, corresponding to the Néel magnetic transition temperature, T_N. The magnetization versus temperature curve indicates a magnetic transition at about 50 K, which is higher than that of MnO_2 nanowires synthesized by a hydrothermal method with a diameter of 20–50 nm (T_N = 13 K). The different grain width effect will possibly explain the difference. This illustrates that MnO_2 has an antiferromagnetic structure with a parasitic ferromagnetic component below the Néel temperature. Figure 8(b) shows the magnetization versus applied magnetic field for MnO_2 after removing the CMK-3 support, from which we can see that the transition peaks are much broader and the magnetisize value is higher for CMK-MnO_2 in comparison with the resultant MnO_2 nanowires because of defects and larger distortion for the confinement of nanoparticles MnO_2 inside mesoporous carbon.[3] Consistently, the M-H curve shows a small hysteresis for the MnO_2 nanowires, which indicates that a ferromagnetic component is superimposed on the antiferromagnetic curve.

IV. CONCLUSION

In conclusion, one-dimensional α-MnO_2 nanowires with a controlled width of 10–20 nm were synthesized from mesoporous carbon by means of ultrasonic waves. During the removal of the carbon wall at elevated temperatures, the nanowires inside the pores occupied the positions of the combusted carbon and aggregated in one-dimension along the original host channel. Magnetization measurements indicate an antiferromagnetic interaction or a spin glass state coexisting with the ferromagnetic state in CMK-MnO_2. A magnetic transition at about 50 K for the sample of MnO_2 nanowires illustrates that MnO_2 has an antiferromagnetic structure with a

CAMBRIDGE JOURNALS
http://journals.cambridge.org Downloaded: 09 Oct 2012 IP address: 130.130.37.84

parasitic ferromagnetic component below the Néel temperature. A major advantage of this approach is the easy, efficient, and reproducible control of width from mesoporous carbon, in addition to the relatively high purity of the resultant. The suggested growth mechanism is in good agreement with our experimental results and may be a general one for the growth of other metal oxide with special properties. This approach is expected to widen the applications of self-ordered mesoporous carbon with a variety of morphologies.

ACKNOWLEDGMENTS

S. Zhu acknowledges the financial support of the National Science Foundation of China (Grant No. 50573013) and the Shanghai Science and Technology Committee (Grant Nos. 05ZR14077 and 06PJ14063). X.L. Wang thanks the Australian Research Council for financial support through ARC Discovery Projects under Grant Nos. DP0345012 and DP0558753. The authors thank SJTU Instrument Analysis Center for the measurements.

REFERENCES

1. Z. Tian, W. Tong, J. Wang, N. Duan, V.V. Krishnan, and S.L. Suib: Manganese oxide mesoporous structures: Mixed-valent semiconducting catalysts. *Science* **276,** 926 (2002).
2. A. Perner, K. Holl, D. Ilic, and M. Wohlfahrt-Mehrens: A new MnO_x cathode material for rechargeable lithium batteries. *Eur. J. Inorg. Chem.* **5,** 1108 (2002).
3. R. Chitrakar, H. Kanoh, Y.S. Kim, Y. Miyai, and K. Ooi: Synthesis of layered-type hydrous manganese oxides from monoclinic-type $LiMnO_2$. *J. Solid State Chem.* **160,** 69 (2001).
4. J-B. Yang, X-D. Zhou, W-J. James, S-K. Malik, and C-S. Wang: Growth and magnetic properties of $MnO_{2-\delta}$ nanowire microspheres. *Appl. Phys. Lett.* **85,** 3160 (2004).
5. Z-W. Pan, Z-R. Dai, and Z-L. Wang: Nanobelts of semiconducting oxides. *Science* **291,** 1947 (2001).
6. A. Govindaraj, B.C. Satishkumar, M. Nath, and C.N-R. Rao: Metal nanowires and intercalated metal layers in single-walled carbon nanotube bundles. *Chem. Mater.* **12,** 202 (2000).
7. J. Sloan, D.M. Wright, H.G. Woo, S. Bailey, A.P.E. York, K.S. Coleman, M.L.H. Green, D.M. Wright, J.L. Hutchison, and H-G. Woo: Capillarity and silver nanowire formation observed in single walled carbon nanotubes. *Chem. Commun.* **8,** 699 (1999).
8. C.M. Lieber: One-dimensional nanostructures: Chemistry, physics and applications. *Solid State Commun.* **107,** 607 (1998).
9. J.J. Urban, W.S. Yun, Q. Gu, and H.K. Park: Synthesis of single-crystalline perovskite nanorods composed of barium titanate and strontium titanate. *J. Am. Chem. Soc.* **124,** 1186 (2002).
10. M. Li, H. Schnablegger, and S. Mann: Coupled synthesis and self-assembly of nanoparticles to give structures with controlled organization. *Nature* **402,** 393 (1999).
11. X-F. Duan, Y. Huang, Y. Cui, J-F. Wang, and C-M. Lieber: Indium phosphide nanowires as building blocks for nanoscale electronic and optoelectronic devices. *Nature* **409,** 66 (2001).
12. X. Wang and Y. Li: Synthesis and formation mechanism of manganese dioxide nanowires/nanorods. *Chem. -Eur. J.* **9,** 300 (2003).
13. Y-J. Han, J.M. Kim, and G.D. Stucky: Preparation of noble metal nanowires using hexagonal mesoporous silica SBA-15. *Chem. Mater.* **12,** 2068 (2000).
14. F. Gao, Q. Lu, and D. Zhao: Synthesis of crystalline mesoporous CdS semiconductor nanoarrays through a mesoporous SBA-15 silica template technique. *Adv. Mater.* **15,** 739 (2003).
15. A.H. Janssen, C-M. Yang, Y. Wang, F. Schüth, A.J. Koster, and K.P. Jong: Localization of small metal (oxide) particles in SBA-15 using bright-field electron tomography. *J. Phys. Chem. B* **107,** 10552 (2003).
16. B. Tian, X. Liu, H. Yang, S. Xie, C. Yu, B. Tu, and D. Zhao: General synthesis of ordered crystallized metal oxide nanoarrays replicated by microwave-digested mesoporous silica. *Adv. Mater.* **15,** 1370 (2003).
17. H. Yang, Q. Shi, B. Tian, Q. Lu, F. Gao, S. Xie, J. Fan, C. Yu, B. Tu, and D. Zhao: One-step nanocasting synthesis of highly ordered single crystalline indium oxide nanowire arrays from mesostructured frameworks. *J. Am. Chem. Soc.* **125,** 4724 (2003).
18. M. Wei, Y. Konishi, H. Zhou, H. Sugihara, and H. Arakawa: Synthesis of single-crystal manganese dioxide nanowires by a soft chemical process. *Nanotechnology* **16,** 245 (2005).
19. A. Dong, N. Ren, Y. Tang, Y. Wang, Y. Zhang, W. Hua, and Z. Gao: General synthesis of mesoporous spheres of metal oxides and phosphates. *J. Am. Chem. Soc.* **125,** 4976 (2003).
20. W. Li, A. Lu, C. Weidenthaler, R. Goddard, H-J. Bongard, and F. Schüth: Growth of single crystal-Al_2O_3 nanofibers on a carbon aerogel substrate. *J. Mater. Chem.* **15,** 2993 (2005).
21. P. Dibandjo, F. Chassagneux, L. Bois, C. Sigala, and P. Miele: Comparison between SBA-15 silica and CMK-3 carbon nanocasting for mesoporous boron nitride synthesis. *J. Mater. Chem.* **15,** 1917 (2005).
22. W. Li, A. Lu, C. Weidenthaler, and F. Schuth: Hard-templating pathway to create mesoporous magnesium oxide. *Chem. Mater.* **16,** 5676 (2004).
23. M. Imperor-Clerc, D. Bazin, M-D. Appay, P. Beaunier, and A. Davidson: Crystallization of β-MnO_2 nanowires in the pores of SBA-15 silicas: In situ investigation using synchrotron radiation. *Chem. Mater.* **16,** 1813 (2004).
24. S. Zhu, H. Zhou, M. Hibino, I. Honma, and M. Ichihara: Synthesis of MnO_2 nanoparticles confined in ordered mesoporous carbon using a sonochemical method. *Adv. Funct. Mater.* **15,** 381 (2005).
25. M. Kruk, M. Jaroniec, C-H. Ko, and R. Ryoo: Characterization of the porous structure of SBA-15. *Chem. Mater.* **12,** 196 (2000).
26. S-H. Joo, S-J. Choi, I. Oh, J. Kwak, Z. Liu, Q. Terasaki, and R. Ryoo: Ordered nanoporous arrays of carbon supporting high dispersions of platinum nanoparticles. *Nature* **412,** 169 (2001).
27. T-D. Xiao, P.R. Strutt, M. Benaiss, H. Chen, and B.H. Kear: Synthesis of high active-site density nanofibrous MnO_2-base materials with enhanced permeabilities. *Nanostruct. Mater.* **10,** 1051 (1998).
28. Z. Liu, Y. Sakamoto, T. Ohsuna, K. Hiraga, O. Terasaki, C-H. Ko, H.J. Shin, and R. Ryoo: TEM studies of platinum nanowires fabricated in mesoporous silica MCM-41. *Angew. Chem., Int. Ed.* **39,** 3107 (2000).

CAMBRIDGE JOURNALS
http://journals.cambridge.org Downloaded: 09 Oct 2012 IP address: 130.130.37.84